Control of Induction Thermal Plasmas by Coil Current Modulation in Arbitrary-waveform

Yuki TSUBOKAWA, Farees EZWAN, Yasunori TANAKA and Yoshihiko UESUGI

Division of Electrical and Computer Engineering,Kanazawa University

Kakuma Kanazawa Ishikawa, 920-1192 Japan

(Received: 1 September 2008 / Accepted: 10 November 2008)

To control temperature and reaction fields in thermal plasmas more effectively, we have recently developed arbitrary-waveform modulated induction thermal plasma (AMITP) system using a high-power semiconductor power supply with metal oxide semiconductor field effect transistors (MOSFETs) and insulated gate bipolar transistors (IGBTs). In this paper, we studied fundamental dynamic behavior of an Ar AMITP from electric and optical approaches. Time evolutions in the effective power and the radiation intensity of Ar lines were measured to understand the dynamic behavior of the AMITP. The Ar excitation temperature was also estimated by the two-line method. Results indicate that the effective power, the radiation intensity and the Ar excitation temperature of Ar AMITP can be changed largely following the coil current modulated by externally given arbitrary-waveform.

Keywords: Modulated induction thermal plasma, MOSFET inverter, PLL control, IGBT dc-dc chopper circuit, temperature control.

1. Introduction

The inductively coupled thermal plasmas (ICTP) is widely used in the material processings, since it has some features of high enthalpy, high radical density, and little impurities[1-3]. However, it often has uncontrollable high enthalpy or high heavy particle temperature which causes thermal damages on the specimen or product in the material processings. To control the temperature of thermal plasmas, we have developed a pulse-modulated induction thermal plasma (PMITP) system [4]. This system modulates the coil current amplitude sustaining an ICTP in a rectangular waveform, and it produces a large periodical disturbance in thermal plasmas. This rectangular modulation of the coil current makes it possible to control the time-averaged temperature, chemical reaction and gas flow fields in thermal plasmas in time-domain.

For further detailed control of temperature and reaction fields in thermal plasmas more effectively, we have recently developed an arbitrary-waveform modulated induction thermal plasma (AMITP) system using a high-power semiconductor power supply with metal oxide semiconductor field effect transistors (MOSFETs) and insulated gate bipolar transistors (IGBTs) [5]. This system controls the coil current amplitude to follow an externally-given arbitrary waveform.

In this paper, we studied fundamental dynamic behavior of the Ar AMITP from electric and optical approaches. The modulated effective power was measured to understand the behavior of the Ar AMITP as a electrical load. Time evolution in the radiation intensity of Ar lines was measured at different axial positions to obtain the fluctuation in the Ar AMITP. The Ar excitation temperature was also estimated by the two-line method. Results indicate that the effective power, the radiation intensity and the Ar excitation temperature of Ar AMITP can be changed following the coil current modulated by externally given different waveforms.

2. Modulated induction thermal plasma

Fig. 1 illustrates a schematic of the coil current for different modulation operations. For a conventional steady operation of ICTPs, the coil current has a fixed amplitude with a fundamental frequency of several hundreds kHz as indicated in Fig. 1 (a). Such a radio-frequency ac variation in the coil current cannot change a heavy-particle temperature in an ICTP because the heavy particle temperature in the ICTP has an inherent response time of the order of milliseconds [6].

Fig. 1 (b) shows the pulse-modulated coil current that we have developed previously [6]. In this case, the current amplitude is changed into a rectangular waveform with a modulation cycle of several tens of hertz. This pulse-modulation of the coil current in milliseconds markedly perturbs thermal plasmas, then the heavy particle temperature of plasmas changes periodically. Setting modulation parameters such as a duty factor and a shimmer current level [6] enables us to control the time-averaged temperature of thermal plasmas.

On the other hand, Fig. 1 (c) indicates an

author's e-mail: 4205tsub@ec.t.kanazawa-u.ac.jp

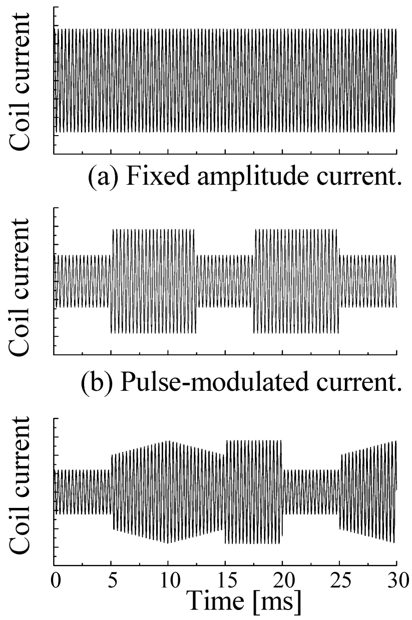

(a) Fixed amplitude current.

(b) Pulse-modulated current.

(c) Arbitrary-waveform modulated current.

Fig. 1 Concept of modulated coil current

arbitrary-waveform modulated coil current. This coil current amplitude is controlled to follow an externally given arbitrary waveform. Such an arbitrary-waveform modulated coil current leads to electric field and effective power. And the effective power leads to more detailed control of the temperature and also reaction fields in thermal plasmas in time domain. It may be possible that controlled coil current in the proper-waveform promotes or limits specified reactions of interest if its reaction rate is much different from others.

3. Experimental setup

3.1 Power supply for arbitrary-waveform modulated induction thermal plasma

Fig. 2 shows the electric circuit of an rf power supply for AMITPs. The power supply consists of four main parts: a three-phase rectifier circuit, an insulated gate bipolar transistor (IGBT) dc-dc converter (chopper) circuit, a metal-oxide semiconductor field-effect transistor (MOSFET) full-bridge inverter, and an impedance matching circuit with a matching transformer and an LC series circuit. The driving frequency of the MOSFET inverter is controlled around 350-450 kHz using a phase-looked-loop (PLL) control to obtain load-impedance matching. The output current of the IGBT dc-dc converter circuit and then the amplitude of the MOSFET output rf current are controlled to fit the waveform of the externally-given modulation control signal using the pulse width modulation (PWM) control method to the IGBT. The modulation control signal is given externally with a programmable function generator.

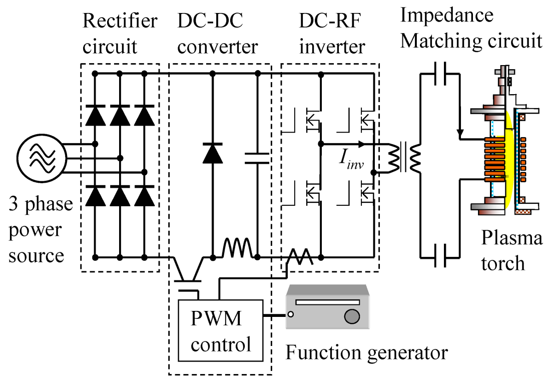

Fig. 2 Electric circuit for AMITP system.

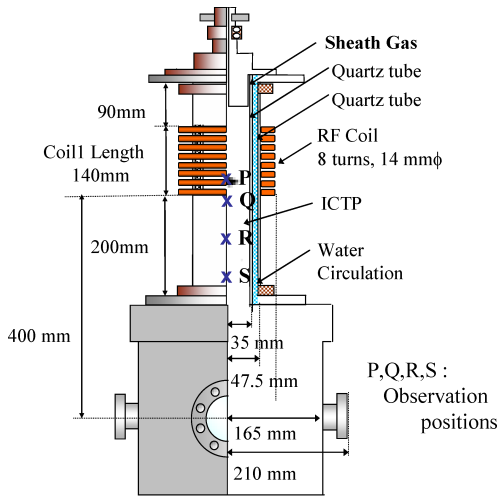

Fig. 3 Plasma torch configuration.

3.2 Plasma torch

Fig. 3 illustrates the plasma torch used in the experiment. The torch is composed of two coaxial quartz tubes with 430 mm length. The inner tube has the interior diameter of 70 mm. Between the inner and outer tubes, cooling water flows from bottom to top side to keep the wall-temperature around 300 K. Argon gas is supplied as a sheath gas along the inner tube wall of the torch with a swirl to prevent the plasma from contacting the inner tube. This torch has an eight-turn induction coil. This coil is connected with an rf power supply with the MOSFET inverter unit through the matching circuit.

3.3 Spectroscopic observation system

Fig. 4 shows the spectroscopic observation system. Spectroscopic observation was carried out between the 6-7th turns of the coil, at 10 mm, 80 mm and 160 mm below the coil-end on the axis of the plasma torch, which are designated by P, Q, R and S in Fig. 3. The observation region at each position is 7 mm in diameter. This region is larger than the 6-7th coil gap of 3 mm, and thus the intensity measured at P is decreased by the limited

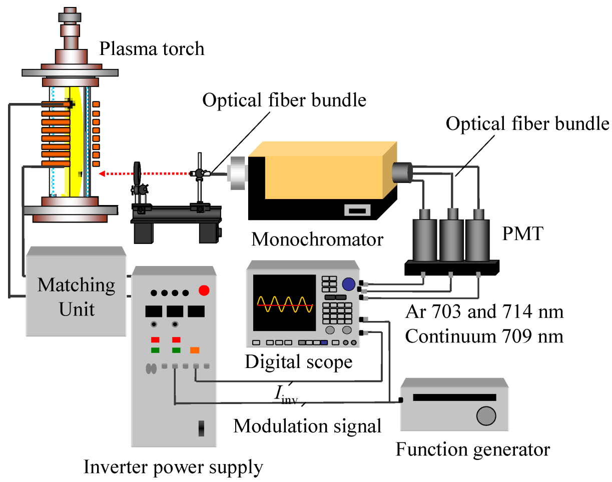

Fig. 4 Spectroscopic observation system.

observation region. The light radiated from the observation positions is transmitted through an optical lens and an optical fiber bundle to the slit of a monochromator. Using this system, time evolution in the radiation intensities at different three wavelengths can be simultaneously measured. In the present experiment, we measured temporal variations in the radiation intensities at 703 nm and 714 nm for Ar lines and 709 nm for continuum. Subtracting the measured radiation intensity at 709 nm from those at 703 and 714 nm yields the net radiation intensities of the Ar atomic lines at 703 and 714 nm. Using the net radiation intensities, Ar excitation temperature between the specified levels was estimated by the two-line method [7]. The above whole optical system was calibrated using a standard tungsten-halide lamp.

3.4 Experimental condition

For establishing an AMITP, we used Ar as a sheath gas. The gas flow rate was 40 slpm (standard liters per minute) for axial gas, and 40 slpm for swirl gas. The pressure was fixed at 200 torr. The input power to inverter circuit was set to 10 kW in any modulation cases.

4. Experimental results

4.1 Coil current and effective power

Fig. 5 shows (a) the modulation signal, (b) the inverter output current in root-mean-square value and (c) the inverter output effective power in a triangular waveform modulation case. The effective power was determined from instantaneous current and voltage measured at the inverter output circuit. As seen in Fig. 5, the coil current of the order of 170 A_{peak} can be modulated according to the triangular modulation signal. The effective power rises slower than the coil current amplitude, which is reflected the thermofluid behavior of AMITP as described later.

The experimental results for a triangle-rectangular modulation are indicated in Fig. 6. This signal was originally programmed and given to the IGBT.

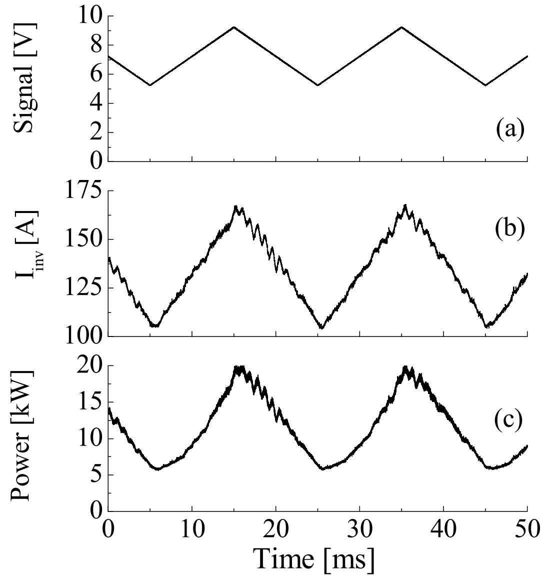

Fig. 5 Time evolution in (a) modulation signal, (b) the inverter output current in root-mean-square value, (c) Inverter output effective power. The coil current amplitude is modulated into a triangular waveform.

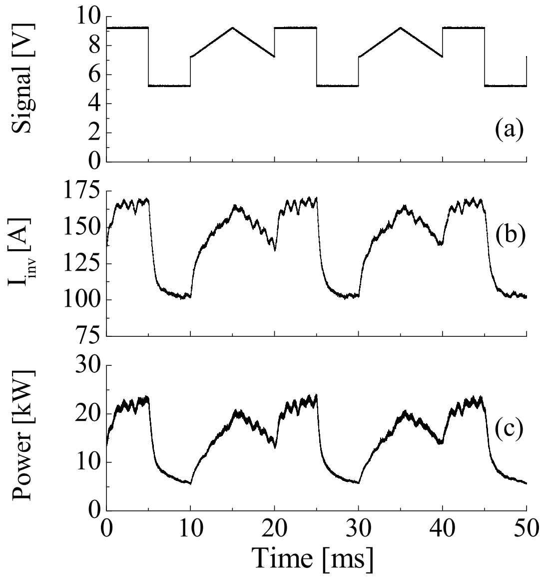

Fig. 6 Time evolution in (a) modulation signal, (b) the inverter output current in root-mean-square value, (c) Inverter output effective power. The coil current amplitude is modulated into a triangle-rectangular waveform.

4.2 Radiation intensity of Ar atomic line

Spectroscopic observation was carried out to find the dynamic behavior of Ar AMITP. Fig. 7 shows (a) the modulation signal, (b) the inverter output current in root-mean-square value, (c) the radiation intensity of the Ar atomic line at 714 nm, and (d) the Ar excitation temperature, in a triangular waveform modulation case. The radiation intensities in Fig. 7 (c) are those of Ar atomic

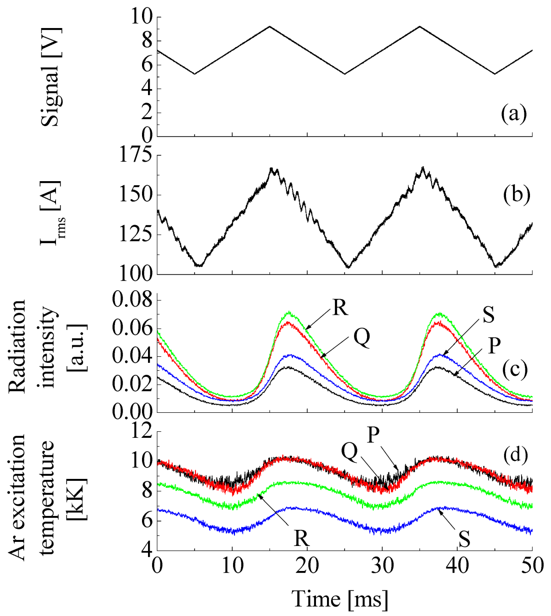

Fig. 7 Time evolution in (a) modulation signal, (b) the inverter output current in root-mean-square value, (c) radiation intensity of the Ar atomic line at 714 nm, (d) Ar excitation temperature from the two-line method. The coil current amplitude is modulated into a triangular waveform.

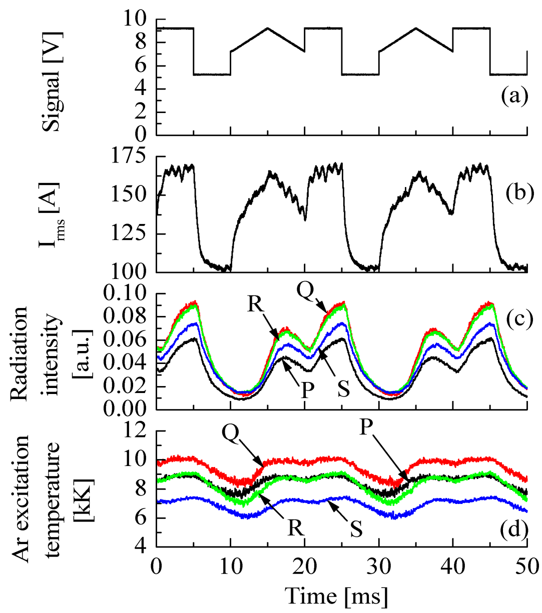

Fig. 8 Time evolution in (a) modulation signal, (b) the inverter output current in root-mean-square value, (c) radiation intensity of the Ar atomic line at 714 nm, (d) Ar excitation temperature from the two-line method. The coil current amplitude is modulated into a triangle-rectangular waveform.

spectral line at 714 nm at different observation positions. It is seen that the radiation intensities are also changed periodically in triangular waveform according to the input effective power for different observation positions. However, there is a delay time found for radiation intensity against the coil current. The delay time was roughly estimated to be 2.5 ms from the time difference between the coil current amplitude peak and the peak of radiation intensities, and 5 ms from the time difference between the minimum of the coil current amplitude and the minimum of the radiation intensity at any observation positions. This delay time in the radiation intensity arises mainly from the thermal inertia of thermal plasmas which is governed mainly by mass density and specific heat of high temperature Ar gas. In addition, the radiation intensity at position R is higher than those observed at P, Q and S in this experimental condition. The intensity at P is the weakest because it is only the one transmitted through the 6-7th coil gap. The higher intensity at Q and R may be attributable to the fact that a Ar plasma is generated inside the coil region and is transported to downstream region by a high axial gas velocity produced. This generation of the plasma in the coil and then convective transport of the plasma may bring the higher intensity at Q and R. Fig. 8 (c) depicts the variation of the radiation intensity for the triangle-rectangular waveform. It is found that the radiation intensity for the rectangular part becomes higher than that for the first triangular part, which is due to the accumulated power input to the plasma.

4.3 Ar excitation temperature

Temperature is one of essential parameters to understand the state of thermal plasmas. In this work, the Ar excitation temperature was estimated by the two-line method using the two specified Ar lines at 703 and 714 nm [7]. Fig. 7 (d) depicts the time evolution in the Ar excitation temperature for the triangular waveform. The Ar excitation temperature can be also changed periodically into a triangular waveform according to the modulation signal for any observation positions. The Ar excitation temperatures measured at positions P and Q change from 8000 K to 10000 K similarly. On the other hand, the Ar excitation temperature at R varies from 7000 K to 9000 K. At further downstream i.e. at position S, Ar excitation temperature changes from 5000 K to 7000 K. As seen above, the absolute value of the temperature decreases to downstream portions at any timing, whereas the temperature waveform are similar and the temperature fluctuation is about 2000 K at any axial observation positions, even at position S. It is also seen that the temperature at position P and Q has a peak value in 16 ms after transition from decreasing current to increasing current, while the temperature at position S reaches a peak in 17.5 ms after the transition. This means that temperature change travels from coil to downstream portion. On the other hand, Fig. 8 (d) shows those for the triangle-rectangular waveform case. The Ar excitation temperatures are also confirmed to change by about

1000-2000 K at any axial positions according to the modulation signal. However, the temperature at position P is lower than at position Q in this triangular-rectangular modulation, which tendency is different from that in case of triangular modulation. This means that modulation shape can change axial temperature distribution in terms of time-averaged value. However, it is noted that the temperature change starts first upstream portions P and Q, and then the temperature at downstream portion R and S changes because of distance from the coil position. In this way, the Ar excitation temperature in Ar AMITP can be controlled by the modulated coil current in milliseconds.

5. Conclusions

In this paper, we studied fundamental dynamic behavior of the Ar AMITP. Time evolution in the coil current and the input effective power to Ar AMITP was measured and found to be modulated periodically following externally given waveform successfully. Spectroscopic observation was carried out to obtain the time-dependent radiation intensity of Ar atomic lines and Ar excitation temperature at different axial positions. The Ar excitation temperature at any axial position can change by 2000 K by a large disturbance in the coil current.

[1] T. Ishigaki et al, Sci. Technol. Advanced Master, 6, 111 (2005).
[2] M. Shigeta et al, Thin Solid Film, 457, 192 (2004).
[3] W. R. Chen et al, Surface Coating Technol., **197**, 109 (2005).
[4] Y. Tanaka et al, IEEE Trans. Plasma Sci., Vol.35, Issue 2, (2007) pp. 197-203.
[5] Y. Tanaka et al, Appl. Phys. Lett, **90**, 071502 (2007).
[6] Y. Tanaka et al, Plasma Sources Sci. Technol., **12**, 69 (2000).
[7] M. Venugopalan, Reactions under plasma conditions, vol. 1, pp. 395-396 (1971), Wilely-Interscience, New York.